

Optimization of the Conditions of Synchrotron Mössbauer Experiment for Studying Electronic Transitions at High Pressures by the Example of (Mg, Fe)O Magnesiowustite

A. G. Gavriiliuk^{a, c, d}, J. F. Lin^b, I. S. Lyubutin^a, and V. V. Struzhkin^c

^a Shubnikov Institute of Crystallography, Russian Academy of Sciences, Leninskĭ pr. 59, Moscow, 119333 Russia
e-mail: lyubutin@ns.crys.ras.ru

^b Lawrence Livermore National Laboratory, Livermore, California 94550, USA

^c Geophysical Laboratory, Carnegie Institution of Washington, Washington DC 20015, USA

^d Institute for High Pressure Physics, Russian Academy of Sciences, Troitsk, Moscow region, 142190 Russia

Received July 5, 2006

The effect of the experimental conditions on the shape of the nuclear resonant forward scattering (NFS) from (Mg_{0.75}Fe_{0.25})O magnesiowustite has been studied at high pressures up to 100 GPa in diamond anvil cells by the method of the NFS of synchrotron radiation from the Fe-57 nuclei at room temperature. The behavior of the system in the electronic transition of the Fe²⁺ ion from the high-spin to low-spin state (spin crossover) near 62 GPa is analyzed as a function of the sample thickness, degree of nonhydrostaticity, and focusing and collimation conditions of a synchrotron beam. It is found that the inclusion of dynamical beats associated with the sample thickness is very important in the approximation of the experimental NFS spectra. It is shown that the electronic transition occurs in a much narrower pressure range (± 6 GPa) rather than in a broad range as erroneously follows from experiments with thick samples under strongly nonhydrostatic conditions.

PACS numbers: 61.50.Ks, 75.50.-y, 76.80.+y

DOI: 10.1134/S0021364006150136

The spectra of the nuclear resonant forward scattering (NFS) of synchrotron radiation from the Fe-57 nuclei in crystals are due to the decay of excited nuclear states into the ground state and constitute a dependence of the intensity of the scattered γ radiation on the time passed since a synchrotron radiation pulse [1]. They are now called synchrotron or time Mössbauer spectra. The damping decay of the nuclear excitation is time-modulated by quantum and dynamic beats determining the shape of the NFS spectra. Quantum beats can be of magnetic and dynamic origins and are caused by the interference between the energies of nuclear sublevels split by the magnetic or/and electric hyperfine interaction. The period of quantum beats is inversely proportional to the hyperfine splitting of nuclear sublevels. Dynamic beats are attributed to the multiple reemission of energy in a “thick” crystal and are determined by the sample thickness. These processes are reviewed in [1].

As a rule, the magnetic and electric quantum beats are easily identified in the experimental NFS spectrum, and they can provide information about the magnitude and direction of the magnetic hyperfine field H_{hf} at the ⁵⁷Fe nucleus and about the magnitude of the electric quadrupole splitting QS [2–5]. However, the shape of the dynamic beats is very similar to the shape of the quantum beats associated with the electric quadrupole

interaction, and this similarity can lead to serious errors in analysis of experimental results.

This paper presents the results of the careful analysis of the NFS spectra of (Mg_{0.75}Fe_{0.25})O magnesiowustite crystals under high pressures in a diamond anvil chamber. It is found that the electronic transition induced by a pressure of about 62 GPa is associated with a change in the spin state of Fe²⁺ ions, but its character depends strongly on the effective thickness of the crystal and the degree of nonhydrostaticity.

EXPERIMENTAL PROCEDURE

Magnesiowustite (Mg, Fe)O has a cubic structure of rock salt and is one of the basic minerals in the lower mantle of the Earth [6]. For this reason, study of its properties at high pressures is important not only for the fundamental physics of strongly correlated electron systems, but also for geophysics. Polycrystalline magnesiowustite samples of the (Mg_{0.75}Fe_{0.25})O composition were synthesized by ceramic technology and contained iron atoms enriched with the ⁵⁷Fe isotope to 96% [7]. For high-pressure measurements, the samples were preliminarily compressed in the diamond cell to plates of various thicknesses and were placed into a working hole of a rhenium gasket with a diameter of about 60 μm . The plate thickness varies from 1 to 13 μm , and

their initial dimension in the plane was from 50 to 80 μm . The spot diameter of the synchrotron radiation beam (measured at the half maximum of the intensity distribution) varied from 5 to 10 μm . A collimator 20 μm in diameter is used in the control experimental run. This made it possible, first, to detect a signal from the central part of the sample, where the pressure gradient is almost absent, and, second, to cut off radiation in the “tails” of the synchrotron radiation beam distribution that can cover the regions of nonhydrostaticity. To measure pressure in terms of the ruby scale, 1–2 μm ruby balls were placed into the working aperture of the diamond cell. The test experiment with the thickest sample (13 μm) was carried out without the medium transferring pressure and without the collimator; for this reason, nonhydrostaticity was maximal in this case. In other experiments, the medium transferring pressure was NaCl. Measurements of the NFS from the ^{57}Fe nuclei at room temperature were conducted on a synchrotron source at the Argonne National Laboratory (United States) on the 16-IDD and 3-IDB beam-lines [8]. The measurement procedure was described in more detail in [7].

PARAMETERS OF THE MEDIUM IN THE CALCULATION OF THE NFS SIGNAL AND THE PARAMETERS OF HYPERFINE INTERACTION AT AMBIENT PRESSURE

Experimental NFS spectra were analyzed by means of the MOTIF program developed by Shvyd'ko [9]. First, it is necessary to calculate (or to experimentally determine) two important parameters of the crystal, the coefficients of absorption μ_{rel} and μ_{res} of photons interacting with electrons (Rayleigh absorption) and with the Fe-57 nuclei (resonance absorption), respectively. These parameters are written in the input MOTIF-a file (motif.27.in) under the numbers 64 for μ_{res} and 65 for μ_{rel} , respectively [9]. With the inclusion of the Mössbauer transition energy $E_\gamma = 14.4125$ keV for the ^{57}Fe nuclei, we obtain $\mu_{\text{rel}} = 0.0083961$ μm^{-1} .

The nuclear absorption is of resonance character and is described by the formula

$$\mu_{\text{res}} = N_0 \sigma_{\text{res}}, \quad (1)$$

where $\sigma_{\text{res}} = 2.5575 \times 10^{-18}$ cm^2 is the cross section for the resonance absorption of Mössbauer photons and N_0 is the concentration of the ^{57}Fe Mössbauer nuclei in the sample. For $(\text{Mg}_{0.75}\text{Fe}_{0.25})\text{O}$, we used the unit cell parameter $a_0 = 4.2450$ \AA from the ICSD database for the $(\text{Mg}_{0.77}\text{Fe}_{0.23})\text{O}$ crystal close in the composition. For N_0 , we obtain

$$N_0 = \frac{4 \times 0.23}{76.50 \times 10^{-24} \text{ cm}^3} = 1.2026 \times 10^{23} \text{ cm}^{-3}. \quad (2)$$

Here, 4 is the number of the sites of the Mg(Fe) ions in a unit cell and 76.5×10^{-24} cm^3 is the unit cell volume.

As a result, according to Eqs. (1) and (2), $\mu_{\text{res}} = 3.07568$ μm^{-1} .

At room temperature and ambient pressure, the Fe^{2+} ions in the $(\text{Mg}_{0.75}\text{Fe}_{0.25})\text{O}$ crystal are in the paramagnetic state, and the ordinary Mössbauer absorption spectrum consists of the quadrupole doublet [10] associated with the splitting of the excited level of the ^{57}Fe nuclei (spin $I = \pm 3/2$) by the inhomogeneous crystal field. The quadrupole splitting $QS = 0.727$ mm/s and isomer shift $IS = 0.614$ mm/s (with respect to the metallic iron) are consistent with the high spin state of the Fe^{2+} ions.

To analyze the NFS spectra at ambient pressure, the indicated parameters of the hyperfine interaction were taken as the initial parameters (zeroth approximation) in the input file motif.27.in of the MOTIF program [9]. Further, the other parameters of the sample were obtained by fitting the calculated NFS spectrum to the experimental data.

OPTIMIZATION OF THE SAMPLE PARAMETERS AND EXPERIMENTAL CONDITIONS

Figure 1 shows the NFS spectra calculated for various values of the effective thickness of the $(\text{Mg}_{0.75}\text{Fe}_{0.25})\text{O}$ sample. It is clearly seen that the shape of the spectrum (the set of beats and their time intervals) is independent of the sample thickness up to a certain value. This is explained by the fact that the effects of self-absorption of γ radiation and dynamic beats are absent for thicknesses smaller than the critical value of about 5 μm . This is the case of pure quantum beats, which are easily calculated and interpreted. With a further increase in the sample thickness, the pattern of the beats loses regularity, dynamic beats appear in addition to quantum beats, and the spectrum is strongly complicated. The calculated and experimental spectra for a thickness of 13.2 μm are shown in the upper part of Fig. 1. Comparison indicates the presence of strong dynamic beats in this sample. However, it is difficult to take into account their effect when calculating the quadrupole splitting parameter QS , which can lead to serious errors in its determination.

We note that, simulating the spectra shown in Fig. 1, the parameter QS was fixed to be equal to the value $QS = 0.727$ mm/s experimentally determined from the Mössbauer absorption spectroscopy (the quantity $2QS \cong 15\Gamma_0$, where Γ_0 is the natural width of the Mössbauer line, which is equal to $\Gamma_0 = 0.097$ mm/s for the ^{57}Fe nuclei, is fixed in the input file).

Since the sample was prepared from a powder, the calculations by the MOTIF program include a procedure taking into account disordering of the electric field gradient vector in direction and averaging with respect to three angles in space. The final theoretical approximation obtained for the NFS experimental spectrum for ambient pressure under the assumption of the presence

of only quadrupole splitting and disordering of the electric field gradient directions is also shown in the upper part of Fig. 1. It is seen that the first half of the spectrum (first maximum) is well reproduced, but then significant discrepancy with experiment is observed. For a fixed quadrupole splitting parameter, the calculated effective thickness of the sample is estimated as $\sim 13.2 \mu\text{m}$, which is close to the thickness determined by optical methods including the porosity of the sample.

Figure 2 shows the sample-thickness dependence of the second-minimum position in the NFS spectra calculated for $(\text{Mg}_{0.75}\text{Fe}_{0.25})\text{O}$ magnesiowustite. According to this figure, for dynamic beats to be absent, the sample thickness should not exceed $3\text{--}4 \mu\text{m}$. Unfortunately, the accumulation time of the NFS experimental spectrum with the same quality in this case should be increased by three or four times.

As seen in Fig. 1, the time interval of measuring the NFS spectrum, which is determined by the time distance between the nearest synchrotron radiation pulses (bunches), is also an important parameter. For an interval of about $\sim 140 \text{ ns}$, which was used in these experiments and which is available at third-generation synchrotrons (APS, Argonne, United States; ESRF, Grenoble, France; SPring-8, Japan), even one total beating (to the second minimum) is present incompletely in the quantum beating regime (Fig. 1) for the given value $QS = 0.727 \text{ mm/s}$. If this time interval is at least doubled, the spectrum accumulation time is doubled.

However, we found that the correct design of the experiment, when the dynamic beats are insignificant, can provide the sufficiently reliable determination of the parameter QS even in a time interval of 140 ns and in the presence of only one minimum in the NFS spectrum in the quantum beating regime.

PRESSURE DEPENDENCE OF THE QUADRUPOLE SPLITTING PARAMETER IN $(\text{Mg}_{0.75}\text{Fe}_{0.25})\text{O}$ WITH THE INCLUSION OF DYNAMIC BEATS

The geometric thickness of the polycrystalline sample in the high-pressure chamber decreases under pressure. However, the sample density increases correspondingly, and the effective ‘‘Mössbauer’’ thickness remains approximately constant. For this reason, when analyzing the NFS spectra of the $(\text{Mg}_{0.75}\text{Fe}_{0.25})\text{O}$ samples, we assume that the change in their shape under high pressure is not caused by change in the thickness and is primarily attributed to change in QS . Figure 3 shows experimental NFS spectra for three $(\text{Mg}_{0.75}\text{Fe}_{0.25})\text{O}$ samples of thicknesses 13 , 5 , and $1 \mu\text{m}$ for various pressures and their theoretical approximation under indicated assumptions. As seen in Fig. 3a, the calculations poorly reproduce experimental data for a sample thickness of $13 \mu\text{m}$, although the dynamic beats are taken into account. The first minimum, which can be used to formally calculate the QS value, is the

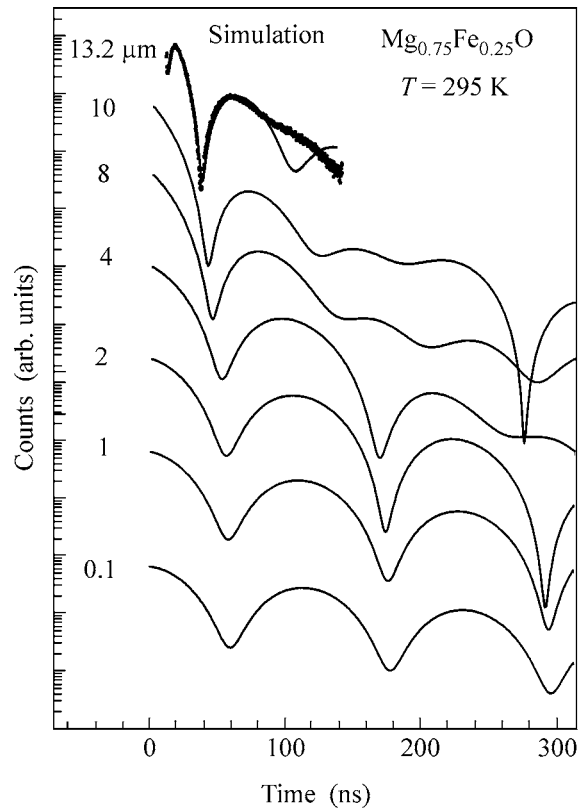


Fig. 1. (Lines) Theoretical spectra calculated for $(\text{Mg}_{0.75}\text{Fe}_{0.25})\text{O}$ for various sample thicknesses and (points) experimental spectra under normal conditions for the sample $13.2 \mu\text{m}$ in thickness.

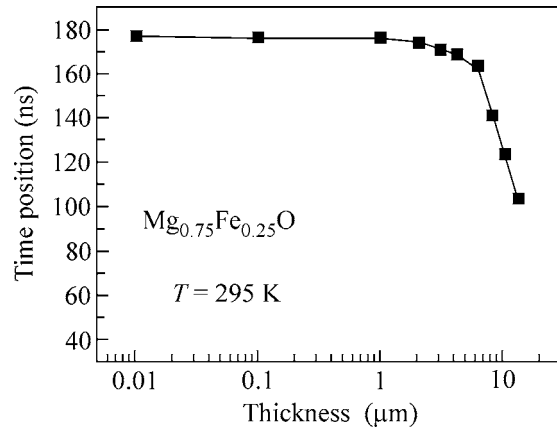


Fig. 2. Sample-thickness dependence of the second-minimum position in the NFS spectra calculated for $(\text{Mg}_{0.75}\text{Fe}_{0.25})\text{O}$ magnesiowustite.

only feature that is described quite reliably. The theoretical approximation is satisfactory for the samples 5 - and $1\text{-}\mu\text{m}$ thick (Figs. 3b and 3c, respectively) and the values obtained for the parameter QS can be considered as reliable.

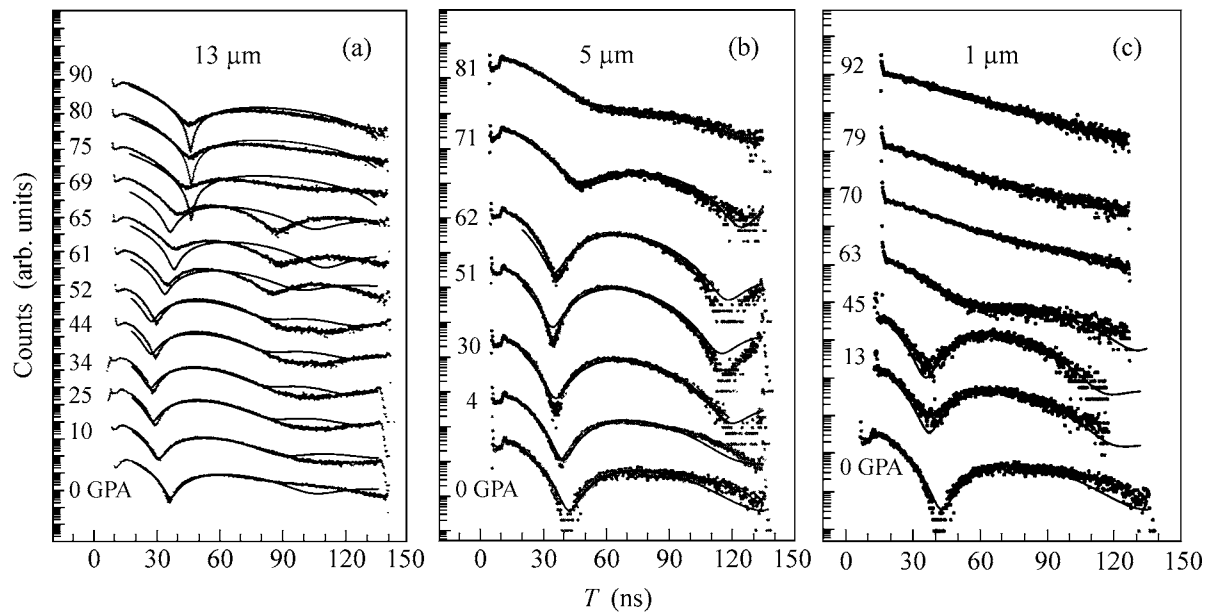


Fig. 3. (Points) Experimental NFS spectra for $(\text{Mg}_{0.75}\text{Fe}_{0.25})\text{O}$ for various pressures and three sample thicknesses 13, 5, and 1 μm and (lines) calculated spectra.

Figure 4 shows the pressure dependence of the parameter QS calculated for samples of various thicknesses that is obtained using the indicated approximation procedure. It is seen that, as the pressure increases near 60 GPa, the parameter QS decreases to zero, which is obviously associated with the rearrangement of the electronic structure and with the transition of the Fe^{2+} ions from the high-spin (HS) to the low-spin (LS) state. However, for the “thick” sample, the mixture of dynamic beats to quantum beats leads to a large error in

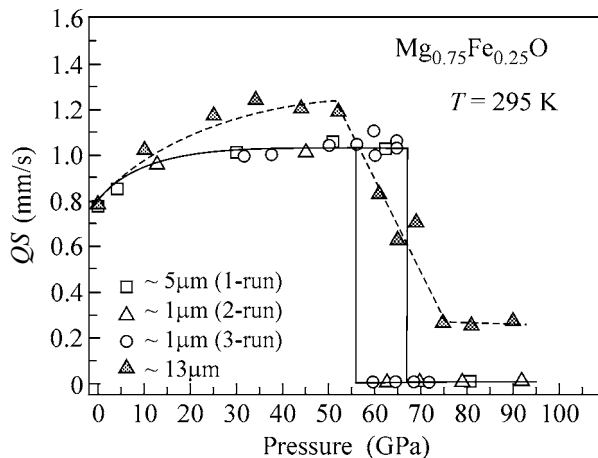


Fig. 4. Pressure dependence of the quadrupole splitting parameter QS calculated for $(\text{Mg}_{0.75}\text{Fe}_{0.25})\text{O}$ from the experiments with the samples of various thicknesses. The dashed lines are guides to the eyes. The solid lines are guide to the eyes and show the intermediate region of the transition.

the determination of the hyperfine parameters. As a result, the observed range of the electronic transition is expanded to 30–50 GPa (Figs. 4 and 5b). According to the measurements on thin samples, actual smearing of this transition is much smaller and is no more than ~ 10 GPa (Fig. 5a). This is a fundamental result of these investigations.

Figure 5 shows the pressure dependence of the high-spin phase content determined from three experiments carried out for various nonhydrostaticity degrees and various sample thicknesses. It is seen that, as the nonhydrostaticity, as well as thickness, of the sample increases, the observed transition width increases strongly. Thus, to obtain reliable results in the high-pressure NFS experiment in diamond anvils, it is necessary (i) to use a soft medium transferring pressure in order to reduce the pressure gradient on the sample, (ii) to use a “thin” sample in order to suppress dynamic beats in the NFS spectrum and to reduce the uncontrolled axial pressure gradient, and (iii) to collimate the synchrotron beam in order to reduce the parasitic signal in the tails of the synchrotron radiation beam.

DISCUSSION

The quadrupole splitting parameter QS is associated with the interaction of the electric field gradient $q = \text{grad}(\mathbf{E})$ with the quadrupole nuclear moment Q . The hyperfine interaction Hamiltonian has the form

$$H = \frac{eqQ}{4I(2I-1)} [3I_z^2 - I(I+1)] + \frac{\eta}{2} (I_+^2 - I_-^2). \quad (3)$$

Here, e is the elementary charge, I is the nuclear spin operator, $I_{\pm} = I_x \pm iI_y$, and $\eta = (V_{xx} - V_{yy})/V_{zz}$ is the asymmetry parameter, where $V_{xx} = \partial^2 V / \partial x^2$, $V_{yy} = \partial^2 V / \partial y^2$, $V_{zz} = \partial^2 V / \partial z^2$, V is the electric field potential, and $|V_{zz}| \geq |V_{xx}| \geq |V_{yy}|$. The eigenvalues of the energy operator QS have the form

$$E_Q = \frac{eqQ}{4I(2I-1)} [3m_l^2 - I(I+1)] \left(1 + \frac{\eta}{3}\right)^{1/2}. \quad (4)$$

In the general case, the electric field gradient q at the ^{57}Fe nucleus is the sum of two basic components, lattice q_{lat} (from the crystal field of the surrounding ion ligands) and electronic q_{el} (from the nonspherical distribution of the charge of the own electronic shell of the iron ion) [11]. For the pure cubic symmetry, $q_{\text{lat}} = 0$.

Our experiment shows that the Fe^{2+} ions in $(\text{Mg}_{0.75}\text{Fe}_{0.25})\text{O}$ magnesiowustite at ambient pressure are in the paramagnetic high-spin ($S = 2$) state and occupy the same type of sites in the crystal lattice, and the QS value is equal to ~ 0.7 mm/s. Taking into account that the lattice contribution q_{lat} to the QS parameter in cubic $(\text{Mg}_{0.75}\text{Fe}_{0.25})\text{O}$ is equal to zero, the observed quadrupole splitting is associated with the electron contribution q_{el} .

The cause of this behavior is as follows. The bivalent iron ions Fe^{2+} with the $3d^6$ configuration in $(\text{Fe}, \text{Mg})\text{O}$ magnesiowustite occupy sites in distorted oxygen octahedra. In the cubic crystal field O_h , the $3d^6$ term is split into the upper orbital doublet 5E and lower orbital triplet 5T_2 , which are separated by the energy gap $10Dq$. The high-spin 5T_2 ($t_{2g}^4 e_g^2$) and low-spin 1A_1 ($t_{2g}^6 e_g^0$) states are possible electronic states. In the ideal cubic surrounding, 5E (doublet) and 5T_2 (triplet) are degenerate. In the high-spin ($t_{2g}^4 e_g^2$) state, two electrons occupy two orbitals on the upper e_g sublevel and four electrons are uniformly distributed over the three orbitals of the lower t_{2g} sublevel. In this case, both contributions q_{lat} and q_{el} must be equal to zero, and the quadrupole splitting is absent [12]. However, orbitally degenerate states are unstable, and the oxygen octahedra can be either slightly compressed or extended due to the Jahn–Teller distortions, which leads to the removal of the degeneracy of these sublevels [11, 13]. Therefore, the upper e_g sublevel is split into two orbitals $|x^2 - y^2\rangle$ and $|z^2\rangle$, whereas the lower t_{2g} sublevel is split into three orbitals $|xy\rangle$, $|xz\rangle$, and $|yz\rangle$. The nonuniform occupation of three orbitals by four electrons on the t_{2g} sublevel is responsible for the considerable electric field gradient q_{el} . This is observed in the experiment for the high-spin state of $(\text{Mg}_{0.75}\text{Fe}_{0.25})\text{O}$.

Transitions between the high-spin and low-spin states are possible when the sublevel splitting energy in

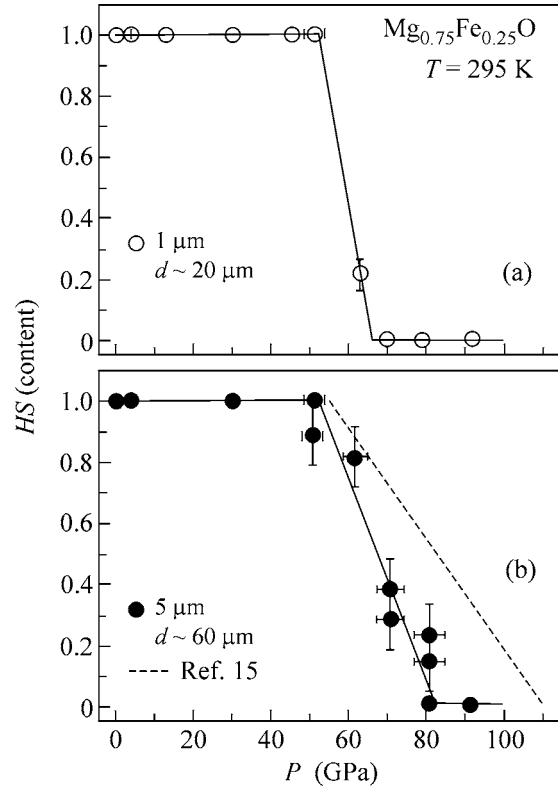


Fig. 5. Pressure dependence of the content of the high-spin phase of the Fe^{2+} ion in the $(\text{Mg}_{0.75}\text{Fe}_{0.25})\text{O}$ sample (a) $1 \mu\text{m}$ in thickness and with an effective diameter of $20 \mu\text{m}$ ($20\text{-}\mu\text{m}$ collimator is used) and (b) $5 \mu\text{m}$ in thickness and with an effective diameter of $60 \mu\text{m}$. In both cases, NaCl is used as a medium transferring pressure. The dashed line is taken from [15], where the entire working volume is densely filled by the sample and the soft medium transferring the pressure is absent.

the crystalline field is comparable with the Hund energy of the interatomic exchange interaction.

As follows from the analysis of the NFS spectra, the quadrupole splitting in magnesiowustite increases from ~ 0.7 to ~ 1.0 mm/s with pressure below 62 GPa, which is likely associated with an increase in distortions of the crystal lattice and electric field gradient at the iron ion nucleus due to the lattice contribution q_{lat} . According to measurements on “thin” samples (see Figs. 3b and 3c), quantum beats completely disappear for pressure above 62 GPa, which indicates that the parameter QS is zero. This can be associated only with a sharp change in the electron spin structure and with the transition of iron ions from the high-spin to low-spin state. In the transition to the low-spin state ($t_{2g}^6 e_g^0$), two electrons transit from the upper e_g level to the lower t_{2g} sublevel. As a result, three sublevels t_{2g} are completely occupied by six electrons whose spins are compensated (diamagnetic state with the spin $S = 0$), and the electron contribution q_{el} to the electric field gradient vanishes. The ground state A_1 of the low-spin phase is stable.

The HS–LS crossover has also been observed in recent investigations of the high-resolution synchrotron x-ray emission Fe- $K\beta$ spectra from the iron atoms in magnesiowustite [14]. In that work, the electronic transition with a change in the spin of the Fe²⁺ ions from $S = 2$ to $S = 0$ is observed in a pressure range of 56–67 GPa.

Thus, we have found that the spin crossover occurs in (Mg_{0.75}Fe_{0.25})O magnesiowustite crystals at a pressure of 62 GPa and room temperature; i.e., iron ions transform from the high-spin paramagnetic state ($S = 2$) to the low-spin diamagnetic state ($S = 0$). The correct inclusion of the dynamic beats in the NFS spectra confirms that this transition occurs in a much narrower pressure range (± 6 GPa) rather than in a broad range (from ~ 50 to 100 GPa) as was erroneously assumed previously [15]. In our opinion, this error is associated with the large thickness (~ 30 μm) of the sample used in [15] and with the high pressure gradient due to the absence of the pressure-transferring medium.

We emphasize that this electronic transition occurs at room temperature when the magnetic order is initially absent in the crystal at ambient pressure; therefore, the HS–LH spin crossover is not accompanied by magnetic collapse as observed, e.g., in the crystals FeBO₃ [2, 3, 16, 17], BiFeO₃ [18], (La, Pr)FeO₃ [19, 20], Fe₂O₃ [21], and Y₃Fe₅O₁₂ [22]. In this case, in terms of the classical concepts, the order parameter (magnetization) is absent in the (Mg_{0.75}Fe_{0.25})O crystal, and such a transition cannot be considered as the magnetic phase transition; however, the electron spin transition is an experimental fact.

We are grateful to Prof. F. Gülich (Mainz, Germany) and Prof. S.G. Ovchinnikov for valuable advices when discussing the results of this work. This work was supported by the Russian Foundation for Basic Research (project no. 05-02-16142-a) and the Division of Physical Sciences, Russian Academy of Sciences (program “Strongly Correlated Electron Systems”). This work at LLNL was performed under the auspices of the U.S. DOE by UC and LLNL under contract no. W-7405-Eng-4.8. J.F.L. acknowledges the support of the Lawrence Livermore Fellowship.

REFERENCES

1. G. V. Smirnov, *Hyperfine Interact.* **123/124**, 31 (1999).

2. I. A. Trojan, A. G. Gavriilyuk, I. S. Lyubutin, et al., *Pis'ma Zh. Éksp. Teor. Fiz.* **74**, 26 (2001) [*JETP Lett.* **74**, 24 (2001)].
3. I. S. Lyubutin, V. A. Sarkisyan, A. G. Gavriilyuk, et al., *Izv. Ross. Akad. Nauk, Ser. Fiz.* **67**, 1018 (2003).
4. A. G. Gavriilyuk, I. A. Trojan, I. S. Lyubutin, et al., *Zh. Éksp. Teor. Fiz.* **127**, 780 (2005) [*JETP* **100**, 688 (2005)].
5. A. G. Gavriilyuk, V. V. Struzhkin, I. S. Lyubutin, et al., *Pis'ma Zh. Éksp. Teor. Fiz.* **82**, 243 (2005) [*JETP Lett.* **82**, 224 (2005)].
6. D. M. Sherman, *J. Geophys. Res.* **96**, 14 299 (1991).
7. J. F. Lin, A. G. Gavriilyuk, V. V. Struzhkin, et al., *Phys. Rev. B* **73**, 113107 (2006).
8. W. Sturhahn, *J. Phys.: Condens. Matter* **16**, S497 (2004).
9. Yu. V. Shvyd'ko, *Phys. Rev. B* **59**, 9132 (1999).
10. G. Shirane, D. E. Cox, and S. L. Ruby, *Phys. Rev.* **125**, 1158 (1962).
11. H. Spiering, E. Meissner, H. Koppen, et al., *Chem. Phys.* **68**, 65 (1982).
12. P. Gülich, in *Chemical Mossbauer Spectroscopy*, Ed. by R. H. Herber (Chapman and Hall, London, 1978), p. 27.
13. H. Koppen, E. W. Muller, C. P. Kohler, et al., *Chem. Phys. Lett.* **91**, 348 (1982).
14. J. F. Lin, V. V. Struzhkin, S. D. Jacobsen, et al., *Nature* **436**, 377 (2005).
15. I. Yu. Kantor, L. S. Dubrovinsky, and C. A. McCammon, *Phys. Rev. B* **73**, 100101 (2006).
16. V. A. Sarkisyan, I. A. Trojan, I. S. Lyubutin, et al., *Pis'ma Zh. Éksp. Teor. Fiz.* **76**, 788 (2002) [*JETP Lett.* **76**, 664 (2002)].
17. A. G. Gavriilyuk, I. A. Trojan, I. S. Lyubutin, et al., *Zh. Éksp. Teor. Fiz.* **127**, 780 (2005) [*JETP* **100**, 688 (2005)].
18. A. G. Gavriilyuk, V. V. Struzhkin, I. S. Lyubutin, et al., *Pis'ma Zh. Éksp. Teor. Fiz.* **82**, 243 (2005) [*JETP Lett.* **82**, 224 (2005)].
19. G. R. Hearne, M. P. Pasternak, R. D. Taylor, and P. Lacorre, *Phys. Rev. B* **51**, 11 495 (1995).
20. W. M. Xu, O. Naaman, G. Kh. Rozenberg, et al., *Phys. Rev. B* **64**, 094411 (2001).
21. M. P. Pasternak, G. Kh. Rozenberg, G. Yu. Machavariani, et al., *Phys. Rev. Lett.* **82**, 4663 (1999).
22. I. S. Lyubutin, A. G. Gavriilyuk, I. A. Trojan, and R. A. Sadykov, *Pis'ma Zh. Éksp. Teor. Fiz.* **82**, 797 (2005) [*JETP Lett.* **82**, 702 (2005)].

Translated by R. Tyapaev